ORIGINAL RESEARCH Open access

Soil Moisture Sensor-Based Automation of Basin Irrigation Using IoT Technology

James Walker[1*], Olivia Harris[1], George Wilson[2]

Abstract

Irrigation accounts for one of the highest uses of freshwater resources across the agricultural industry. Among various techniques, surface irrigation is one of the most popular choices because of its straightforward implementation and minimal energy consumption. Yet, it is commonly linked to reduced irrigation application efficiency, largely resulting from excessive deep percolation and irregular water spread. A research trial was conducted in a closed-end level basin setup on loamy soil to design and assess an Internet of Things (IoT)- based framework that wirelessly connects an automatic check gate to soil moisture sensors. This setup enables remote management depending on current soil moisture readings. Efforts focused on finding the optimal sensor position in the basin to improve irrigation application efficiency. An aluminium automatic check gate, mounted within an iron frame, was installed within the concrete supply channel to regulate water flow. Three capacitance-based soil moisture sensors were positioned at 25%, 50%, and 75% of the field length (i.e., 15 m, 30 m, and 45 m) and at depths of 37.5 cm, 15 cm, and 7.5 cm, respectively. Wireless links were created between the capacitance-based soil moisture sensors and the automatic check gate via LoRa and GSM modules. Croplytics® by Agsmartic served as the software for automatic regulation of the check gate during this investigation. The setup was tested over nine irrigation cycles on bare soil. Three varied operational plans, each tied to different sensor locations, were examined at 40%, 30%, and 20% soil moisture deficit levels. Outcomes showed that the optimal sensor spot for shutting the system is at 37.5 cm depth, located at 25% of the length from the inlet, under greater soil moisture deficit, while at 7.5 cm depth at 75% of the length under lower deficit conditions. In total, automation increased irrigation application efficiency to 86.6%.

Keywords Internet of Things (IoT), Automation, Basin irrigation, Soil moisture sensor, Wireless communication, LoRa

*Correspondence:
James Walker
james.walker@ed.ac.uk
[1] Department of AI for Autonomous Weeding Robotics, Faculty of Agriculture, University of Edinburgh, Edinburgh, United Kingdom
[2] Department of Machine Learning for Herbicide Resistance Tracking, Faculty of Agriculture, University of Leeds, Leeds, United Kingdom

Introduction

Water scarcity makes its management one of the biggest challenges in arid and semi-arid zones. Proper water management, along with higher water-use efficiency, is a highly effective approach for protecting water supplies, especially in irrigated agriculture. Agriculture represents the biggest user of freshwater [1, 2]. Better irrigation efficiency can conserve significant water, which can then be used to irrigate new areas. Surface irrigation remains the dominant practice for watering crops and pastures worldwide, thanks to its cost-effectiveness and reduced energy requirements [3]. It contributes significantly to food and fodder availability in India. As an illustration, it was applied to roughly 80% of all irrigated land during 2016-2017 [4]. Still, such systems typically exhibit modest water-use efficiency and substantial labor requirements [1, 5].

This is an open access article distributed under the terms of the Creative Commons Attribution-NonCommercial-ShareAlike 4.0 International License (CC BY-NC-SA 4.0), which permits non-commercial use, distribution, reproduction, and adaptation in any medium or format, provided that appropriate credit is given to the original author(s) and source, a link to the license is provided, and any changes made are indicated. Adapted material must be distributed under the same license.

© 2025 The Author(s). | Published by Agro Intelligence Research Press

Properly planned and supervised surface irrigation setups can reach elevated application efficiencies [6]. Nonetheless, the majority of existing surface irrigation operations run at much lower and inconsistent efficiency rates. Surface irrigation is projected to keep its leading position both globally and within India in the years ahead [7]. As a result, continuous efforts to improve the efficiency of surface irrigation applications are anticipated. Factors impacting irrigation outcomes fall into three main groups: field geometry (length, width, slope, and furrow shape), field conditions (infiltration rates and surface roughness), and management factors (flow rate, cut-off timing, and soil moisture deficit before irrigation) [8]. Additional efficiency improvements require real-time adjustments to inflow rates and irrigation cut-off periods for each event to match actual field conditions better. Research findings have shown that application efficiency might grow by 20% just through doubling the inflow rate in basin or border check irrigation for pasture and fodder crops in northern Victoria, Australia [9, 10].

An IoT-based automation approach could be valuable for upgrading traditional surface irrigation practices. Automated surface irrigation means operating the system with timers, sensors, computers, or mechanical tools, with minimal human input. Several studies have shown that deploying intelligent controllers and wireless sensor networks in irrigation systems can achieve water conservation of up to 38% [11, 12]. Automation offers an intelligent way to tackle excessive labor use and inefficient water application in surface systems. A range of soil moisture sensors—tensiometers, gypsum blocks, granular matrix sensors, time-domain reflectometers, and dielectric probes—is commercially available. These can support either manual monitoring or integration into automatic control through IoT platforms [13-15]. The sensor identifies the advancing water front and signals to halt the flow. In basin irrigation, efficiencies over 90% are achievable when the appropriate irrigation length is selected to limit tailwater runoff [9]. A tested automated system using wireless soil moisture sensors in a sage crop field over 136 days achieved 90% water savings compared to standard practices in the area [16]. Employing one Bay Drive—a remotely controlled gate actuator—for irrigation automation reduces the time required to manage water levels and flow in paddy cultivation [17]. Within India, canal irrigation networks often deliver uneven water access from head to tail reaches. Manual gate operations at outlets commonly create large gaps between actual supply and demand [18]. Field-level automation of check gates can address such imbalances through real-time control [19].

IoT is a network of physical items equipped with electronics, software, sensors, and connectivity that enable them to collect and transfer data. This technology helps farmers apply up-to-date tools to overcome major monitoring and workforce shortages. Emerging low-cost IoT solutions are advancing agriculture by improving output quality, volume, long-term viability, and economic returns. An IoT automation platform works by detecting conditions, processing information, exchanging data, and driving physical equipment to perform actions such as valve or gate operation, based on needs or timing [20]. Sensors paired with actuators are fundamental elements of IoT architectures. In full automation, sensor data is sent directly to the actuator for immediate response.

In contrast, in semi-automation, it is routed first to a central controller before actuator commands are issued. Full automation uses less energy overall, but semi-automation simplifies expansion with additional sensors by avoiding the need for custom coordination algorithms [21]. Actuator effectiveness depends on reliable communication, coordination with the controller, and especially adequate power availability. In setups with multiple actuators, synchronization becomes essential. While numerous commercial options for sensors, actuators, processors, and communication components exist, they must be energy-independent and affordable—a key concern in farming areas facing electricity constraints [22]. Systems benefit from inexpensive, readily available parts that enable fast setup and simple servicing. Tests on various module combinations for communication and processing, judged by data transfer, cost, and energy use, found LoRa achieving 1000 m versus 150 m for Wi-Fi, with the Arduino Uno showing lower consumption than Raspberry Pi units [23]. Multiple studies confirm that IoT platforms combined with wireless sensor networks using Zigbee or LoRa can regularly transmit field parameters, such as soil moisture and temperature, to enable mobile app-based irrigation scheduling across different crops [24, 25]. IoT, along with WSN, has been successfully applied to various farming activities, including water quality monitoring, intelligent irrigation, data analysis, pest management, and disease tracking [26-34]. Many irrigation types, from drip and sprinkler to surface methods, can be automated with timers, sensors, or mechanical components. This framework begins with preset soil moisture targets for the field. Sensors send updates to the server at set intervals

© 2025 The Author(s). | Published by Agro Intelligence Research Press

via the microcontroller. Once moisture falls below the set limit, the microcontroller starts irrigation until the desired level is restored [35].

Given the existing issues and the potential benefits of IoT-driven automatic irrigation, a prototype system featuring an automated check gate, communication links, and a motor actuator for real-time basin irrigation control was built and evaluated under bare-soil conditions. The automated check gate could be used at outlets in canal irrigation systems.

Sensor positioning and the right count of soil moisture sensors play major roles in determining the success, reliability, and economic value of sensor-driven surface irrigation automation. This topic still requires deeper investigation. Hence, the study set up an experiment to build an IoT-enabled, wireless, automatic basin irrigation system driven by soil moisture sensors to improve field application efficiency. In addition, work was done to establish proper placement, depth, and quantity of sensors working alongside an automatic check gate in basin fields. Such details could help facilitate broader adoption of automated water distribution in canal irrigation networks.

Materials and Methods

Experimental site

The trial took place at the Research Farm of ICAR-Indian Agricultural Research Institute (IARI), New Delhi, spanning September to December 2020 on bare soil **(Figure 1)**. This research plot lay at 28° 37′ 55” N latitude and 77° 09′ 36” E longitude and sat at an average height of 230 m above mean sea level. The soil type in the test area was loam, showing a bulk density of 1.55 Mg m−3. Field capacity was 35.8% (v/v), and the wilting point was 15.5% (v/v). The basic infiltration rate reached 6 mm/h, measured using a double-ring infiltrometer. The closed-end basin irrigation setup covered dimensions of 60 m × 14 m.

© 2025 The Author(s). | Published by Agro Intelligence Research Press

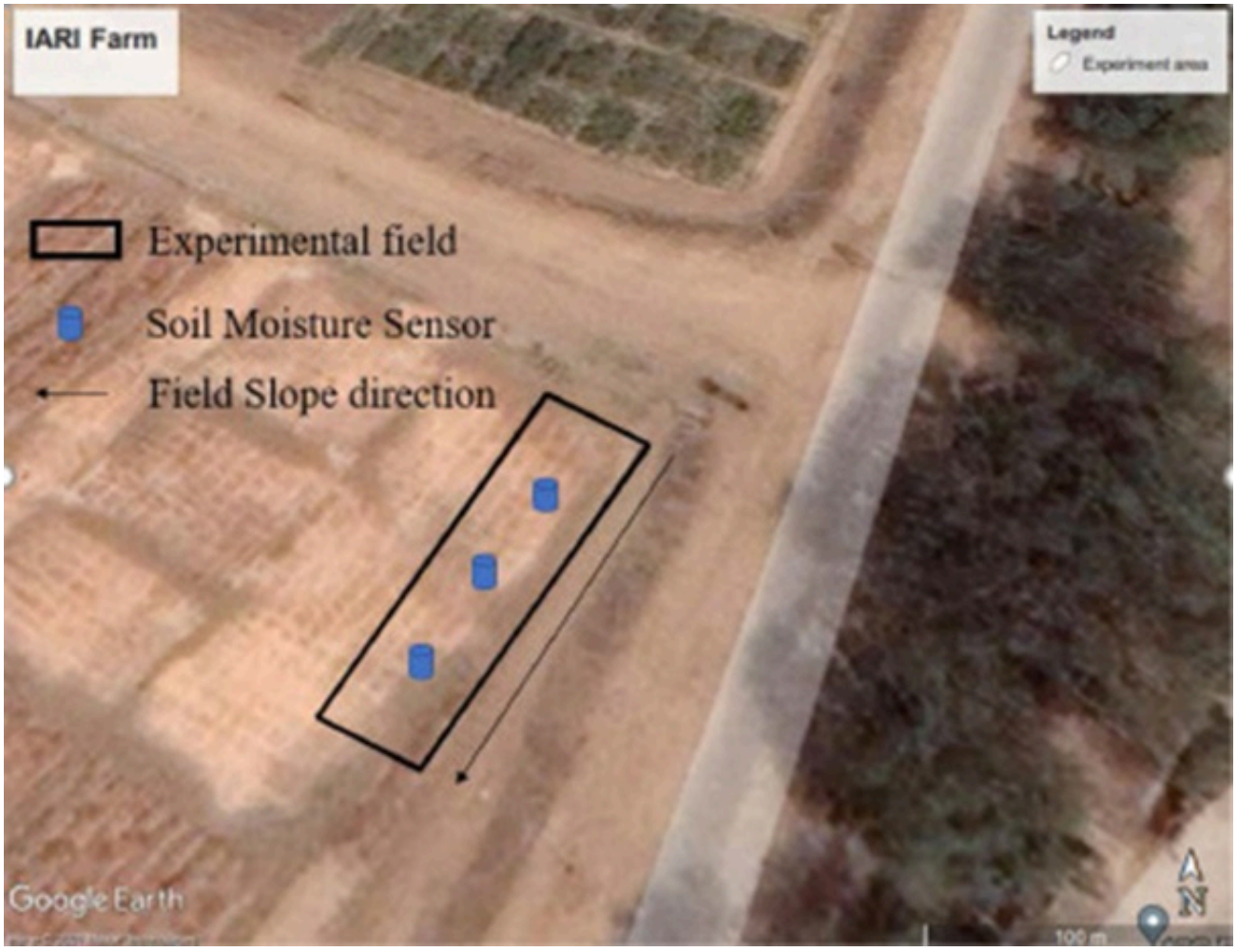

Figure 1. Location map (Google Earth) of the study area at the research farm, IARI, New Delhi.

Components of an automatic irrigation system

Hardware components

A solar-powered automatic check gate controls water entry into the field and remains wirelessly connected to the soil moisture sensors positioned throughout the basin. This gate opens or closes on its own using preset sensor readings to support live control during irrigation events. Constructed from a 7.4 mm aluminium sheet attached to an iron frame, the gate sits at the entry point to the test field inside the supply channel. Rubber seals helped block any water seepage from the edges of the aluminium sheet. Gate opening height measured 30 cm. It was built to function strictly in completely open or completely closed positions. Full technical details of the gate appear in **Figure 2a**. A small solar panel, control box, and solar charging unit were attached directly to the gate. Power supply linked to a 12V DC motor/actuator plus the controller assembly.

Inside the controller sat a voltage converter, a motor driver module, an ultrasonic distance sensor module, an Arduino Nano microcontroller, and a global system for mobile (GSM) module **(Figure 2b)**. Hardware details and roles within the controller unit are listed in **Table 1**. The control box stayed protected inside a sturdy metal casing against rainfall and accidental damage. An ultrasonic sensor was added inside the control box to stop the gate from colliding with the bottom during closure or the upper limit during opening. A metal plate sat right under the ultrasonic sensor to act as a fixed target for tracking gate movement heights. Ultrasonic elements release brief high-frequency sound bursts periodically; upon striking an object, these bursts bounce back as echoes. The sensor determines the distance by measuring the time

© 2025 The Author(s). | Published by Agro Intelligence Research Press

between sending the pulse and receiving the return signal. The metal plate served as the target object, reflecting the pulse so the system could compute its distance. Programming sets the gate to open and close at maximum distances of 20 cm and 50 cm from the ultrasonic sensor. Three buttons on the control box handled power switching, mode selection (automatic or manual), and manual gate lifting or lowering. Power came from a 12 V, 7 Ah battery, charged by a 10 W solar panel. The 10 W, 12 V polycrystalline solar panel proved enough to recharge the 12 V battery. A charge controller displayed overload warnings, charging progress, and low-battery alerts to maintain reliable performance.

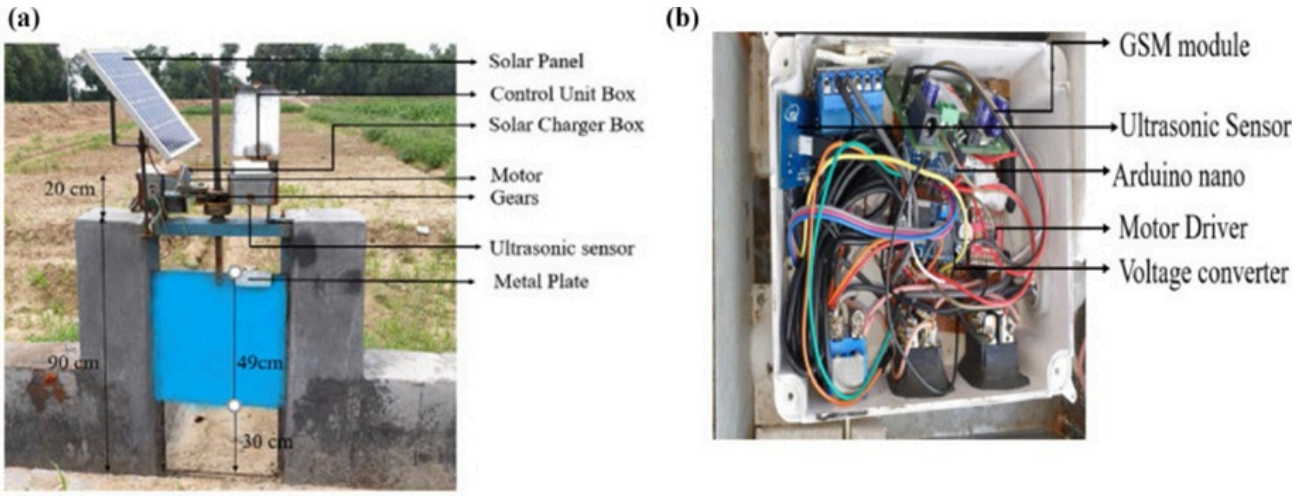

Figure 2. Specifications of the check gate and different components inside the control unit box.

Table 1. Specifications, description, and function of the hardware placed inside the controller unit.

S.No.	Sensor/Module	Model	Specifications	Purpose
1	Motor Driver	A4988 Driver	• Operating supply voltage: 8–35 V • Output current without heatsink: 1 A • Output current with heatsink: 2 A • Logic input voltage: 3–5.5 V	Used for controlling and driving the motor gears
2	Ultrasonic Sensor	JSN-SR04T / JSN-SR04T-2.0	• Operating voltage: 3.0–5.5 V DC • Operating current: < 8 mA • Measurement accuracy: ±1 cm • Acoustic frequency: 40 kHz • Detection angle: < 75° • Operating temperature range: −20 to 70 ℃	Measures the gate opening and closing depth
3	Microcontroller Board	Arduino Nano V3.0	• Controller: Atmel ATmega328 SMD package • Logic operating voltage: 5 V • Digital I/O pins: 14 (6 support PWM) • Analog input pins: 8 • DC per I/O pin: 40 mA • Flash memory: 32 KB (2 KB occupied by bootloader) • SRAM: 2 KB • EEPROM: 1 KB • Clock frequency: 16 MHz	Controls the opening and closing of the gate using moisture data
4	LoRa Module	HPD Tek HPD13A1.1V	• Frequency band: 868 MHz • Supported modulation: FSK/GFSK/MSK/LoRa • SPI communication interface • Receiver sensitivity: −136 dBm • Transmission power: +20 dBm • Data transmission rate: < 300 kbps	Transfers soil moisture information to the gateway

© 2025 The Author(s). | Published by Agro Intelligence Research Press

5	Voltage Converter	LM2596 DC–DC Buck Converter	• Input voltage range: 3.2–40 V DC • Output voltage range: 1.25–35 V DC	Converts a 12 V input supply to a 5 V output
6	Solar Charger Module for Soil Moisture Sensor	CN3065 18650 Li-Ion Mini Solar Charger Board Module	• Input voltage: 4.4–6 V • Charging current: 500 mA • Connector type: 2-pin JST connector (PH2.0 compatible) • Equipped with short-circuit protection • Continuous charging current capability: up to 500 mA	Recharges the Li-Ion battery
7	Microcontroller	ATMEGA328P-U	• Minimum operating voltage: 2.7 V • Maximum operating voltage: 5.5 V • Number of I/O pins: 23 • Number of timers/counters: 3 • 8-bit MCU architecture • Program memory capacity: 32 kB • SRAM size: 2 kB • EEPROM size: 1024 B • Communication interfaces: I2C, SPI, USART	Executes and processes various algorithms
8	Solar Panel	Green Power	• Rated power: 10 W • Output voltage: 12 V	Charges the 12 V battery
9	GSM Module	Simcom SIM800A Quad Band GSM Module	• Supported bands: GSM 850 MHz, EGSM 900 MHz, DCS 1800 MHz, PCS 1900 MHz • 5 V interface support • Required supply voltage: 9–12 V DC with minimum 2 A peak current capability • Operating temperature: −40 ℃ to +85 ℃	Enables communication with the cloud server

Software component

Croplytics® software from Agsmartic was employed for automation in this work and tailored to suit the experimental goals. It features both web-based and mobile interfaces for remote access from any place. The platform displays sensor positions on Google Maps, delivers live soil moisture updates, and manages gate ON/OFF settings tied to selected soil moisture limits. Entering the sensor's global positioning system (GPS) data lets users quickly locate sensors, even in expansive areas. Programming was done in C and C++. Every 3 min, the GSM module uploads soil moisture readings to a designated server, though the interval can be adjusted as required. Shorter gaps increase energy demand. Built-in GSM support allows checking system status remotely via the web or mobile apps at any time. Login credentials are required to access system details **(Figure 3)**.



© 2025 The Author(s). | Published by Agro Intelligence Research Press

Figure 3. Screenshot of Croplytics® (a) web and (b) mobile-based app.

Activation or shutdown of the automatic check gate is possible through web or mobile applications. Sensor information and gate parameters are viewable in the soil moisture and irrigation sections. Graphs showing daily changes in soil moisture, plus data exports for the chosen timeframes, are available in the web version. Minimum and maximum soil moisture threshold values must be entered to run gate operations **(Figure 4)**. These can be adjusted based on each crop's water demand and permitted depletion levels. Once soil moisture reaches or exceeds the chosen limit, the motor driver activates the gate opener. When moisture reaches 90% of field capacity, the gate begins to shut. Maximum soil moisture depletion limits can be set per crop situation. A block diagram and the process flowchart for the automated surface irrigation steps are shown in **Figure 5**.

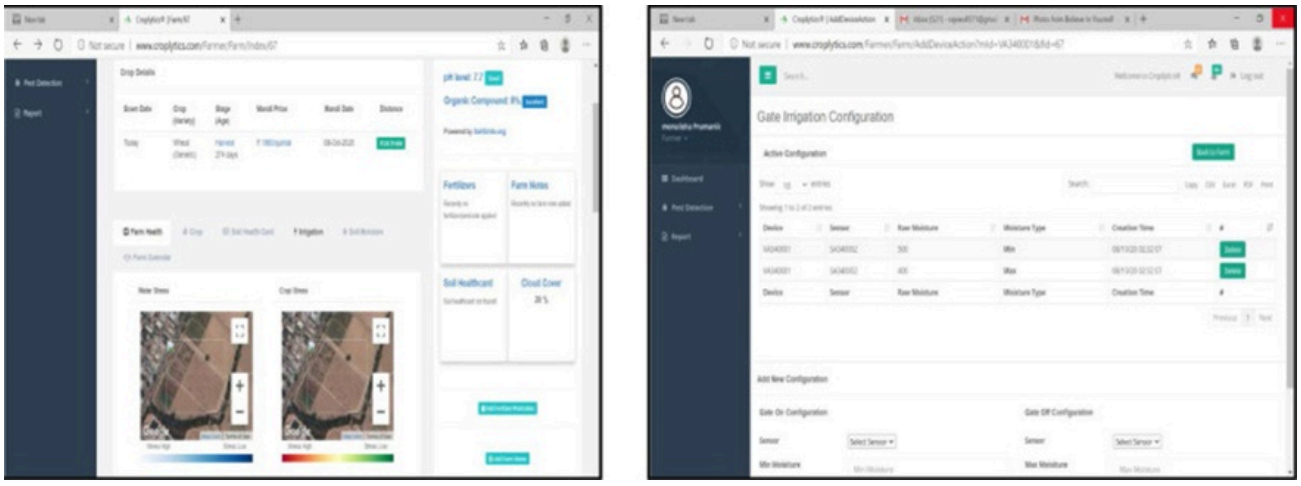

Figure 4. Soil moisture tab and gate configuration tab in Croplytics® web system.

© 2025 The Author(s). | Published by Agro Intelligence Research Press

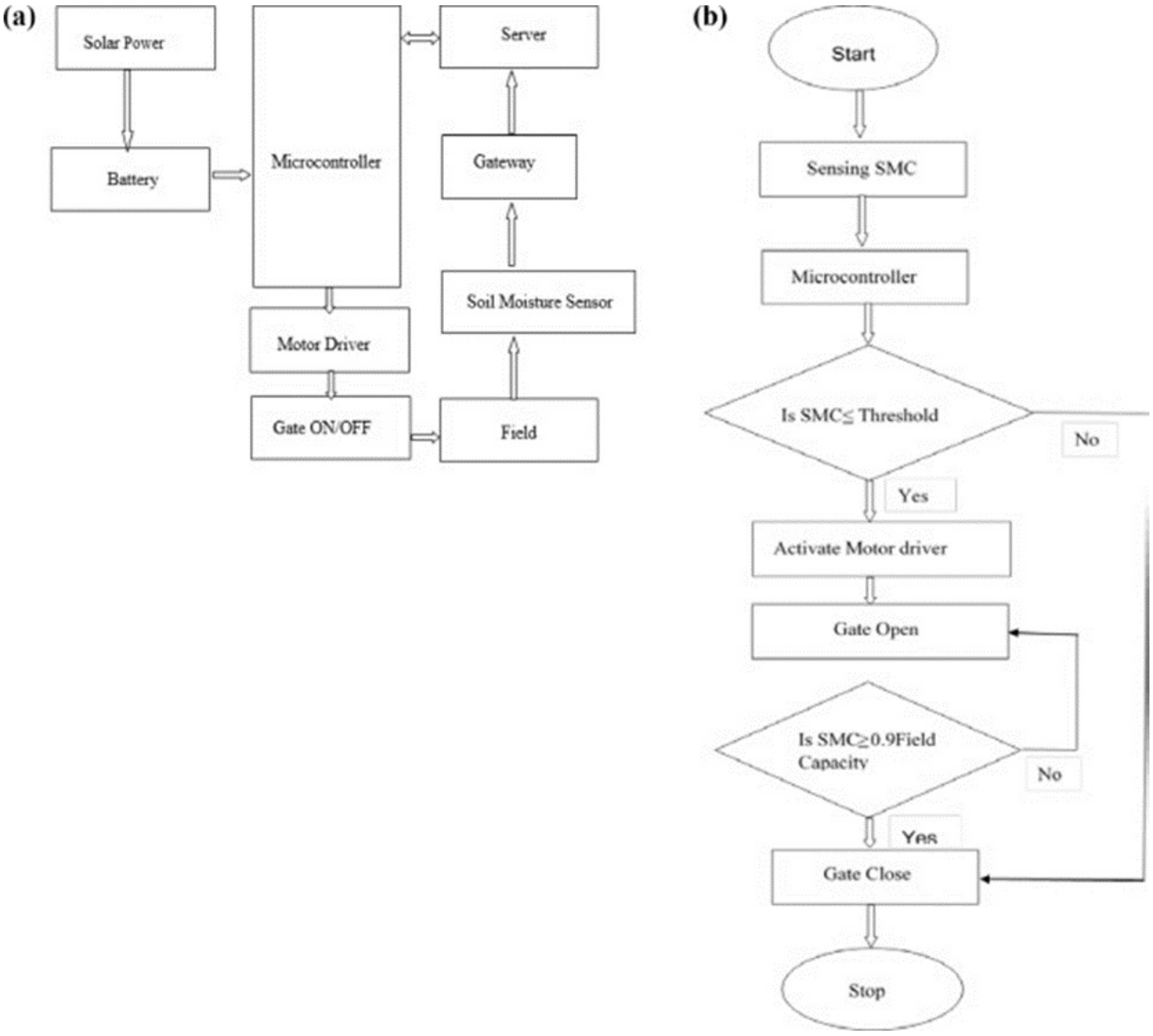

Figure 5. Block diagram and flow chart of the automatic surface irrigation system.

Capacitance-based soil moisture sensor

This sensor measures the dielectric constant difference between soil and water. Electrodes avoid direct soil contact, providing better corrosion resistance than standard resistance sensors. The main parts include the positive plate, the negative plate, and the separating space, called the dielectric. Sharp contrasts in dielectric values between dry soil and water allow clear identification of moisture. A 555 timer circuit assessed sensor capacitance and produced voltage levels matching those of the soil-embedded capacitor **(Figure 6)**. An analogue-to-digital converter (ADC) then converted the voltage to digital form. An inverse relationship exists between voltage and soil moisture: rising voltage signals falling moisture levels. This low-priced, energy-efficient capacitor sensor delivers sufficient precision and is widely used in intelligent automated irrigation systems. It consists of PVC piping, a solar panel, and a circuit enclosure. Model V1.2 runs on low voltage between 3.3 and 5 V, suiting low-power microcontrollers, and uses a three-pin connection. An analogue output pairs well with the Arduino Nano via its ADC. Inside the control enclosure is a 3.7 V Li-Ion battery supported by a top-mounted 5 V solar panel for steady operation. The circuit enclosure houses a microcontroller, a LoRa module for wireless communication, and a solar charging unit with a 3.7 V 8800 mAh Li-Ion rechargeable battery. Microcontrollers are compact, budget-friendly computing devices featuring processors, memory types (ROM, RAM, EPROM), serial

© 2025 The Author(s). | Published by Agro Intelligence Research Press

connections, and timing peripherals for targeted operations. Choice depended on needed precision, processing speed, storage, and specific duties.

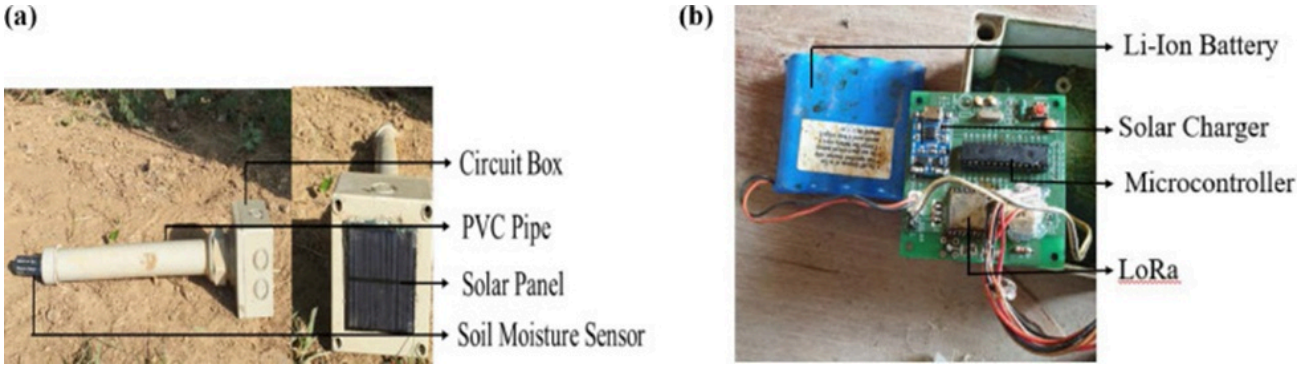

Figure 6. Capacitance-based soil moisture sensor (a) external component and (b) internal components of the circuit box.

Wireless communication network

A key feature of every IoT device is its ability to exchange information and share data with other devices. IoT devices mainly depend on wireless technologies for interaction. A wireless communication network is a network that transmits data through the air using electromagnetic waves, including Infrared (IR), radio frequency (RF), and satellite signals, without requiring any physical wired links. IoT devices may connect using internet-based or non-internet-based protocols, depending on factors such as coverage area, energy usage, and memory needs. Non-Internet protocols require less memory and consume less power within a confined range. Various network protocols exist for different purposes, for instance, ZigBee, Hypertext Transfer Protocol (HTTP), Wi-Fi, Bluetooth, and Long-Range Wide Area Network (LoRaWAN). In the present study, a wireless communication network was created linking the soil moisture sensors, gateway, cloud server, and automatic check gate, as depicted in **Figure 7**. A gateway functions as an intermediary between two separate networks employing distinct transmission protocols. It may operate in unidirectional or bidirectional mode, depending on the direction of data movement. It interprets sensor data and converts it to a suitable format before forwarding it to the cloud network. The gateway was positioned 100 m from the soil moisture sensors and supplied with AC power via a 6 A adapter. The gateway includes a microcontroller, a LoRa module, a global system for mobile (GSM) module, and a buck converter **(Figure 8)**. The LoRa module serves as a wireless communication component for transferring data between sensors and the gateway over extended ranges. It supports low-rate data transmission over an unlicensed radio spectrum. In India, LoRa communications utilize the 865 MHz to 868 MHz frequency band. Its ability to cover long distances (15–20 km) and its minimal power usage make it well-suited for Internet of Things (IoT) applications in agriculture. It applies spread-spectrum technology across a wider bandwidth. The frequency-modulated chirp incorporates coding gain to improve receiver sensitivity. The gateway, cloud server, and automatic check gate were interconnected using a Global System for Mobiles (GSM) module. The SIM800A Quad-Band GSM/GPRS Module with RS232 Interface was chosen for its widespread use and energy-efficient operation. The SIM800A supports Quad-band 850/900/1800/1900 MHz and enables voice, SMS, and data transmission at low power.

© 2025 The Author(s). | Published by Agro Intelligence Research Press

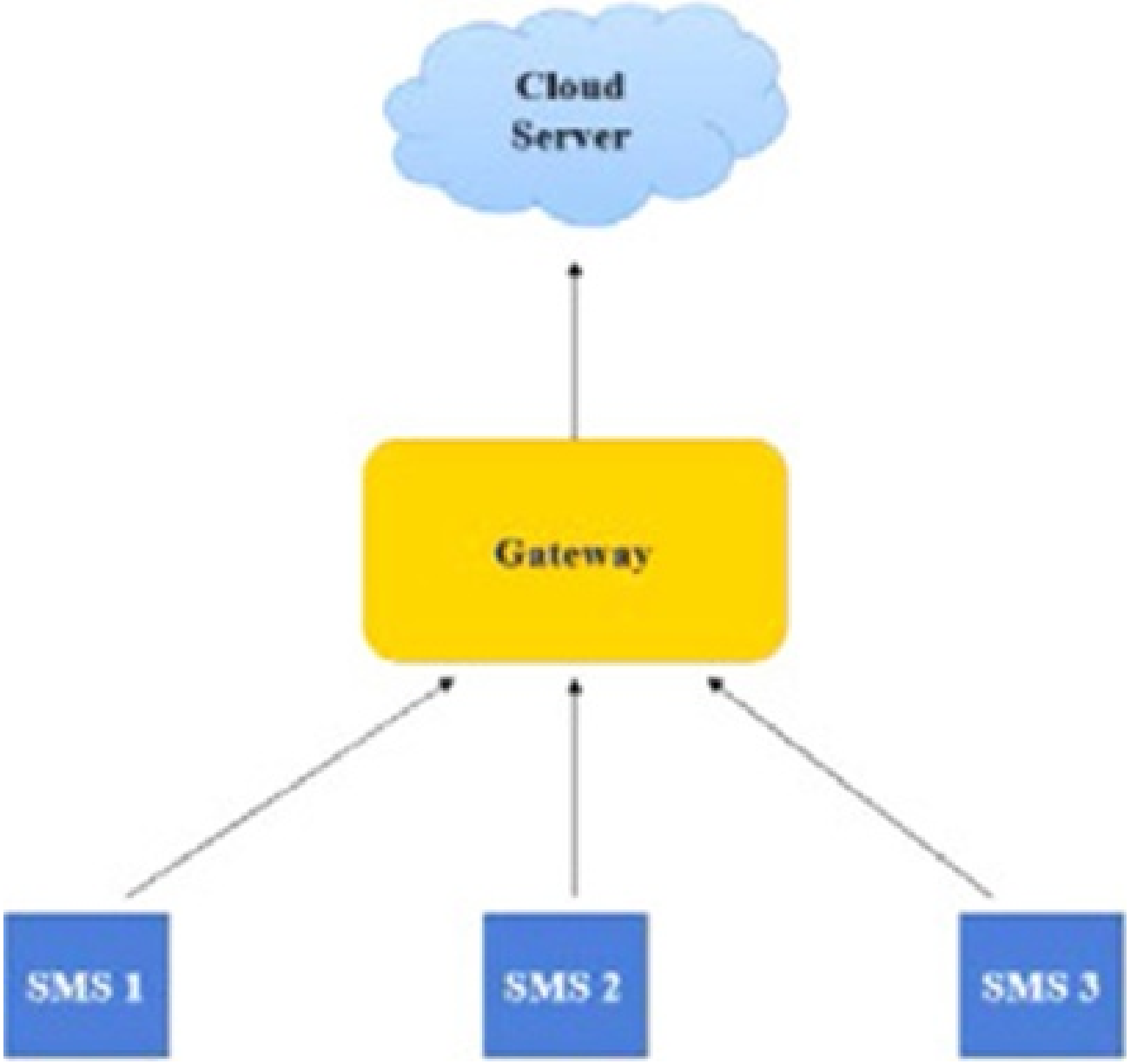

Figure 7. Wireless communication between soil moisture sensors (SMS) and check gate.

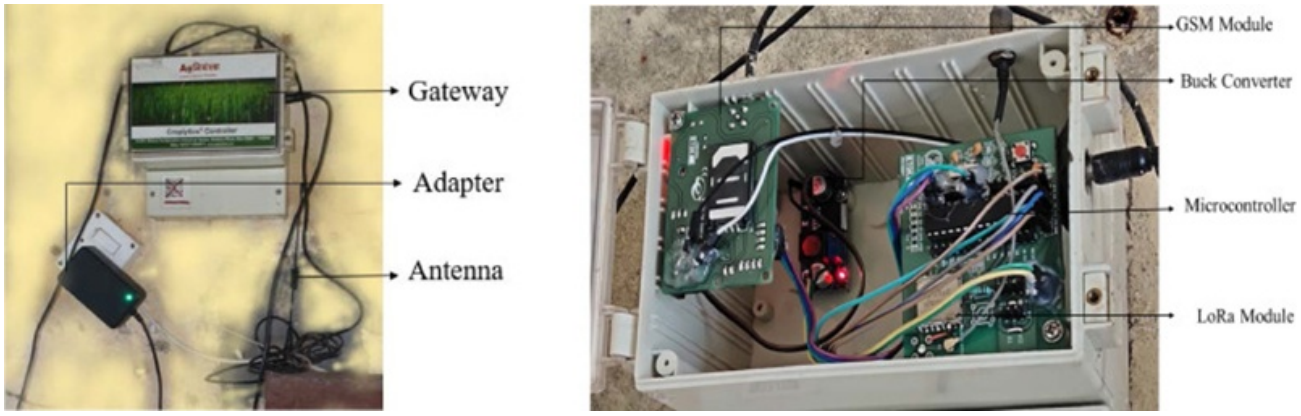

Figure 8. Gateway and its different components.

© 2025 The Author(s). | Published by Agro Intelligence Research Press

The gateway acquired soil moisture data at a 3-min interval via the LoRa module. The system switched to sleep mode during the intervals to conserve energy. Afterward, the data is uploaded to the designated cloud server and relayed to the gate via GSM. Users can program the automatic check gate to operate within specified maximum and minimum soil moisture levels based on crop needs.

Experimental Layout

The experimental basin layout measures 60 m × 14 m and features a 0.0005 m/m slope. Three capacitance-based soil moisture sensors were installed at 25%, 50%, and 75% of the field length, positioned at soil depths of 37.5 cm (Sensor number 1), 15 cm (Sensor number 2), and 7.5 cm (Sensor number 3), respectively. The field inlet included a solar-powered automatic check gate installed in the water supply channel to regulate the beginning and ending of water inflow into the basin. An ultrasonic flow meter (Model Unidata 6526E) was fitted at the inlet for flow rate measurement. The layout of the experimental plot is shown in **Figure 9**.

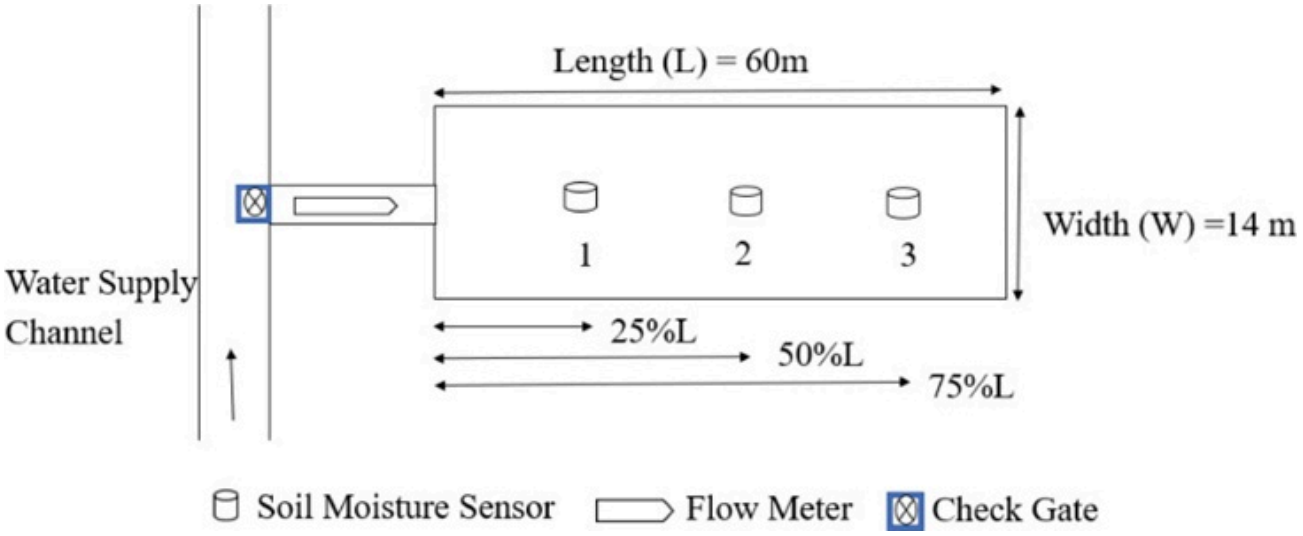

Figure 9. Layout of the experimental field with the placement of the soil moisture sensor and check gate.

Calibration of soil moisture sensor

The soil moisture sensors were calibrated before field deployment. Thirteen soil samples were collected at random from locations with varying moisture levels, from very dry to wet, while sensor readings were recorded. Soil moisture was assessed through the gravimetric method. After measuring fresh weight, the samples were dried in an oven at 105 ºC for 24 h. Soil moisture content was calculated using **Eq. 1**.

$$\theta_g = \frac{(m_{wet} - m_{dry})}{m_{dry}} \times 100 \quad (1)$$

Where, ɵg is the gravimetric soil moisture content (%), mwet and mdry are the fresh and dry weight of soil (g), respectively. Gravimetric soil moisture content was then converted to volumetric soil moisture content using **Eq. 2**.

$$\theta_v = \frac{\theta_g \times \rho_{soil}}{\rho_{water}} \quad (2)$$

Where ɵv is the volumetric soil moisture content (%), ρsoil and ρwater are soil and water density, respectively.

© 2025 The Author(s). | Published by Agro Intelligence Research Press

The digital values recorded by the sensor ranged from 620 in dried soil (θv = 15.5 %) to 384 in saturated soil (θv = 42%). An exponential correlation was identified between volumetric soil moisture content and the sensor's digital value, showing a strong coefficient of determination (R2 = 0.827) **(Figure 10)**.

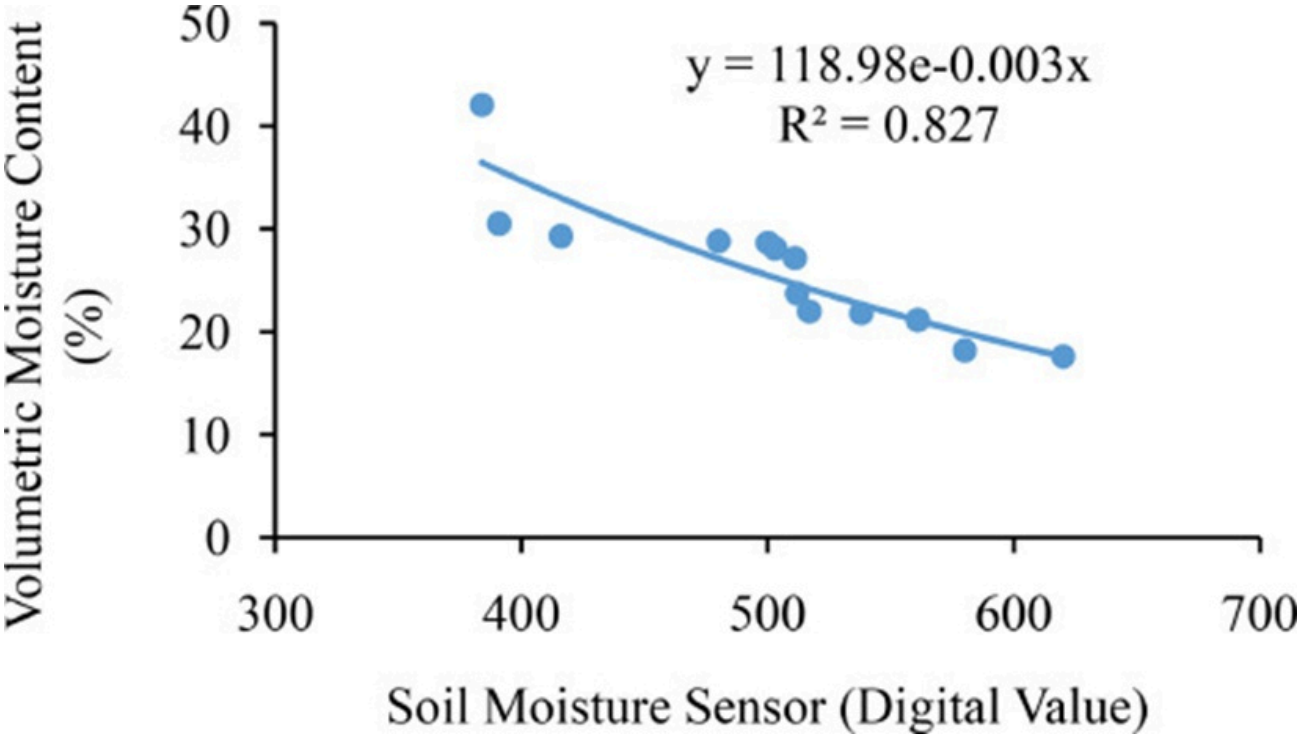

Figure 10. Relationship between volumetric soil moisture content and the digital value of the soil moisture sensor.

Soil moisture sensor placement

Placement of the soil moisture sensor (SMS) was determined based on two main criteria: crop root zone depth and water flow reach, classified into head, mid, and end sections. Sensor depths were adjusted depending on the crop root zone depth and flow reach. The setup was prepared specifically for cultivating wheat during the rabi season (December to April). Multiple combinations of sensor depth (z) and distance (x) were evaluated to determine the optimal positioning for automated surface irrigation **(Table 2)**. Three SMSs were installed at soil depths of 37.5 cm, 15 cm, and 7.5 cm, located at 25%, 50%, and 75% of the field length (L), respectively, to track soil moisture in the head, middle, and end sections of the basin layout **(Figure 11)**.

Table 2. Placement of soil moisture sensors in the field at different depths.

Soil moisture sensor	Distance, *x* (m)	Depth, *z* (cm)
SMS 1	15 (25%L)	37.5
SMS 2	30 (50%L)	15.0
SMS 3	45 (75%L)	7.5

© 2025 The Author(s). | Published by Agro Intelligence Research Press

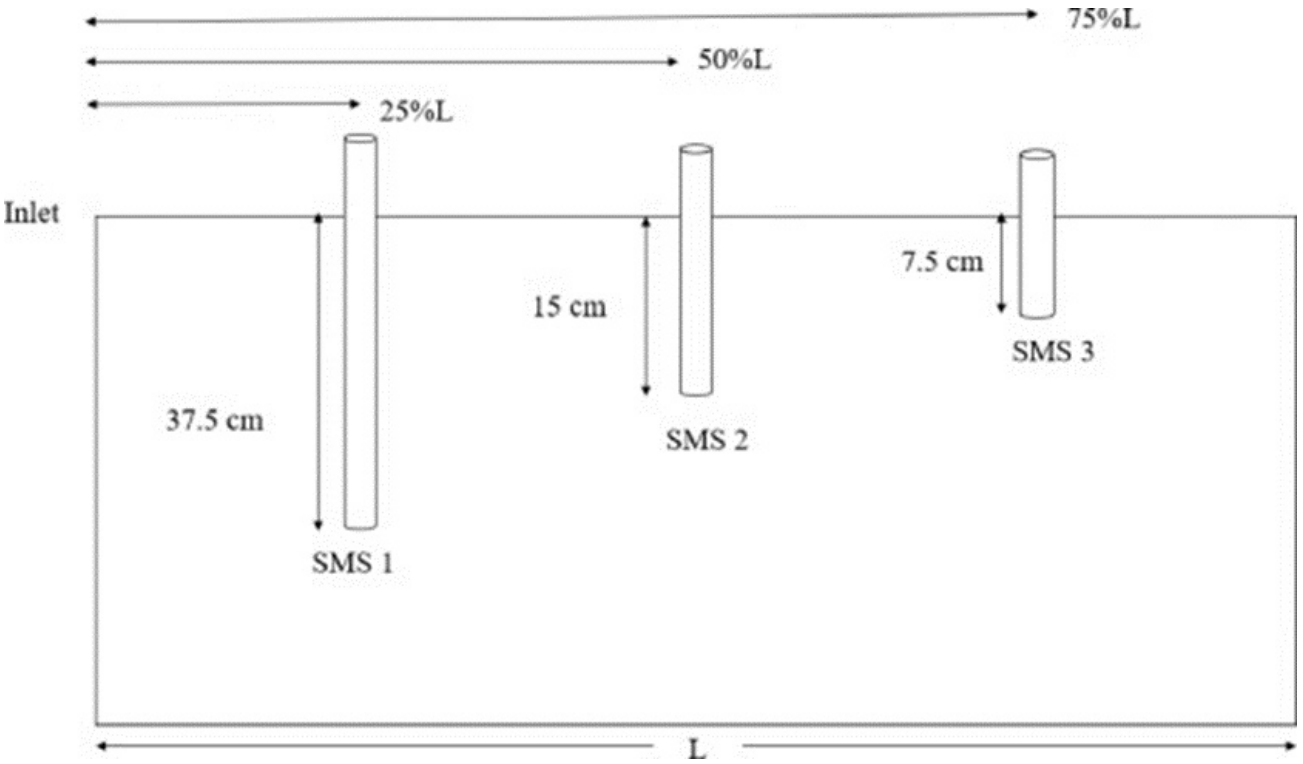

Figure 11. Soil moisture sensor (SMS) placement in the field.

Irrigation management

Operation of the check gate relies on current real-time soil moisture levels. The check gate opens once the preset threshold for soil moisture sensor number 2 is met or surpassed, corresponding to 40%, 30%, and 20% soil moisture depletion from field capacity. The gate closes when the soil moisture content reaches 90% of the field capacity for the specific sensor. Details of the three distinct operational schedules for gate closure are provided in **Table 3**.

Table 3. Description of different operational schedules of the automatic check gate.

Operational schedule (OS)	Description
OS1	The gate closes based on the readings from soil moisture sensor 1 positioned at a depth of 37.5 cm.
OS2	The gate closes according to the measurements obtained from soil moisture sensor 2 located at 15 cm.
OS3	The gate closes in response to data from soil moisture sensor 3, installed at a depth of 7.5 cm.

Irrigation system performance

The complete irrigation system performance was examined using irrigation performance indicators along with the effectiveness of the automatic check gate in sustaining the desired water status within the field.

Irrigation performance indicators

© 2025 The Author(s). | Published by Agro Intelligence Research Press

Three established performance indicators—irrigation application efficiency, low-quarter distribution efficiency, and water requirement efficiency—were applied to assess irrigation performance.

Irrigation application efficiency (Ea)

Irrigation application efficiency represents the proportion of water stored in the crop root zone relative to the total water supplied to the field. The total volume of water delivered in each irrigation event was recorded with an ultrasonic flow meter (Model Unidata 6526E) positioned in the channel immediately downstream of the gate. Irrigation application efficiency was computed using **Eq. 3** [36].

$$E_a = \frac{V_s}{V_a} \times 100 \quad (3)$$

Where Ea is irrigation application efficiency, Vs is the amount of water stored in the root zone, and Va is the volume of applied irrigation. Vs was determined before each irrigation event using the formula where θi is the mass water content before irrigation, ρi is the bulk density, and Zi is the depth of the soil layer in cm for the ith layer.

Distribution uniformity (DUlq)

Distribution uniformity assesses the evenness with which water reaches the designated zone. The low-quarter DU (DUlq) is the mean of the lowest 25% of samples, divided by the overall mean of all collected samples. Greater DUlq values indicate superior uniformity throughout the evaluated zone. Soil samples were collected after each irrigation event from a 10 m × 4.5 m grid to evaluate distribution uniformity. DUlq was computed via **Eq. 4** [37].

$$DU_{lq} = \frac{Average\ of\ the\ lowest\ 1/4}{Average\ of\ all} \times 100 \quad (4)$$

Water requirement efficiency (WRE)

Water requirement efficiency (WRE) gauges the extent to which the field suffered from insufficient irrigation. This metric consistently shows 100% whenever the full field achieves complete irrigation coverage. WRE was derived through **Eq. 5** [38].

$$WRE = \frac{Average\ depth\ of\ root\ zone\ storage}{Average\ depth\ of\ potential\ storage} \times 100 \quad (5)$$

Results and Discussion

Irrigation performance

Testing of the automatic irrigation setup was conducted on bare soil using multiple soil moisture threshold settings. Three operational schedules received monitoring to examine system effectiveness. Each schedule involved tracking three separate irrigation events under bare-field conditions. Key hydraulic details from the irrigation events are shown in **Table 4** and **Figure 12**. The gate opened to full extent and closed completely upon reaching the preset threshold in every case. Opening the gate required 80 s, while full closure took 70 s. Throughout all events, the check gate activated and deactivated on its own exactly when the designated soil moisture level was attained or crossed.

Table 4. Details of the irrigation events under bare-soil conditions.

© 2025 The Author(s). | Published by Agro Intelligence Research Press

Operational schedule (OS)	Water requirement efficiency (%)	Distribution uniformity (DUlq)	Irrigation application efficiency (%)	Volumetric moisture content (%)		Soil Moisture Depletion (%)	Date of irrigation (dd-mm-yy)
				Gate Close	Gate Open		
OS 1	100	0.96	93.0	34.1	27.6	≥40	04.09.20
	100	0.92	92.8	33.4	29.6	≥30	20.09.20
	100	0.82	83.3	33.2	31.6	≥20	10.09.20
OS 2	94.1	0.87	89.8	35.0	27.6	≥40	05.10.20
	91.2	0.84	84.7	35.3	29.6	≥30	22.10.20
	89.5	0.82	83.3	34.9	31.6	≥20	27.10.20
OS 3	86.4	0.78	81.6	34.3	27.6	≥40	20.11.20
	89.2	0.84	82.3	35.5	29.6	≥30	04.11.20
	97.1	0.91	88.6	34.3	31.6	≥20	11.11.20

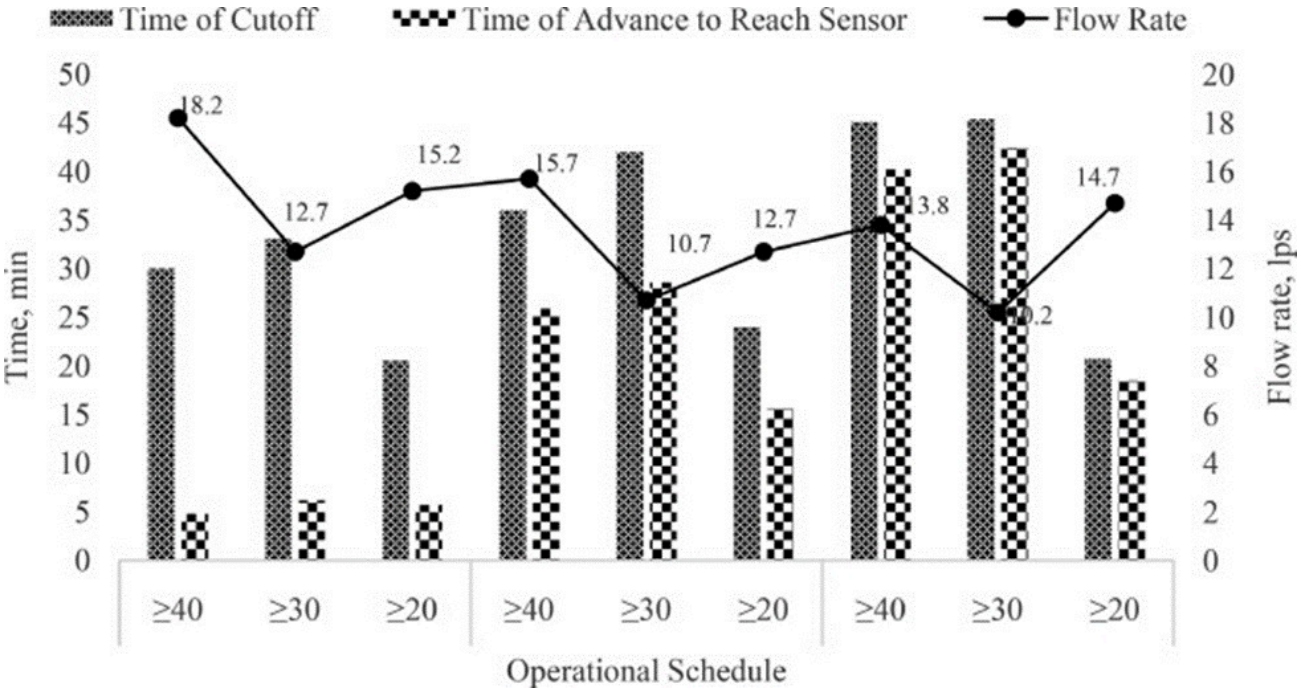

Figure 12. Hydraulic parameters of nine irrigation events.

Under the first operational schedule (OS 1), irrigation began as soon as soil moisture depletion reached 40%, 30%, and 20% of field capacity (FC). Flow rates fluctuated between 12.7 and 18.2 lps. Waterfront arrival times at soil moisture sensor (SMS) number 1 were 4.8, 6.2, and 5.7 min, with corresponding cut-off times of 30, 33, and 21 min for the 40%, 30%, and 20% FC levels. Maximum figures for irrigation application efficiency, distribution uniformity, and water requirement efficiency stood at 93.1%, 0.96, and 100%, respectively, during 40% depletion of FC **(Table 4)**.

© 2025 The Author(s). | Published by Agro Intelligence Research Press

For the second operational schedule (OS 2), flow rates ranged from 10.7 to 15.7 lps, and cut-off durations ranged from 24 to 42 min. Waterfront arrival at the soil moisture sensor (SMS2) occurred at 25.9, 28.6, and 15.6 min for 40%, 30%, and 20% depletion levels, respectively. The leading application efficiency emerged at 40% FC depletion, then 30%, and lastly 20%. In the third operational schedule (OS 3), flow rates ranged from 10.2 to 13.6 lps, and cut-off times ranged from 21 to 45 min. Superior irrigation application efficiency and distribution uniformity were observed at 20% soil moisture depletion, whereas peak water requirement efficiency was observed at 40% depletion.

Time intervals between the sensor's waterfront arrival and cut-off were 22.3, 10.6, and 3.5 min for OS 1, OS 2, and OS 3, respectively. Given the sensor's 37.5 cm depth, water penetration duration proved to be longest under OS 1. Findings revealed that OS1 surpassed the remaining schedules at 40% and 30% depletion, despite recording lower distribution and water-use efficiency. This outcome stemmed from premature threshold triggering for closure in the 20% depletion scenario (sensor positioned at 37.5 cm depth and 15% field length). The diminished uniformity implied by under-irrigation affected one quarter of the field. OS3 displayed a parallel outcome at 40% depletion. Subpar distribution and water requirement efficiencies confirmed that the preset value (90% of field capacity) was activated too soon, before complete field coverage (sensor at 7.5 cm depth and 75% length).

The indicators for irrigation performance — irrigation application efficiency, distribution efficiency, and water requirement efficiency — showed higher values at 40% depletion in OS1 and OS2 than in OS3. This points to larger soil moisture shortfalls boosting surface irrigation outcomes. In total, OS 1 emerged as the top performer across the three schedules. The indicators pointed toward optimal sensor siting for gate closure at the head reach (25% L from inlet) and at a 37.5 cm depth during substantial deficits, shifting to 7.5 cm depth and 75% L from inlet in milder deficit situations. Maximum deep percolation took place at the basin's head section [39]. Consequently, cutting deep percolation losses in the upper area can markedly raise application efficiency [5]. Parallel outcomes were reported by Amiri *et al.* [40], suggesting that sensor depths of 10–20 cm are suitable for automated drip systems for maize. Across the nine events, the averages were 86.6% application efficiency, 0.90 distribution uniformity, and 94.2% water requirement efficiency. These figures highlight automation as a potent strategy for upgrading surface irrigation delivery. Soil moisture shortage levels exert a major influence on system results and correct sensor positioning.

Table 5. Cost of different components of an automated irrigation system.

S. No.	Component	Cost (US$)
1	**Check the gate and controller unit**	
a.	Gate with supporting frame	40.0
b.	GSM communication module	10.7
c.	Motor driver	1.3
d.	Ultrasonic sensing unit	9.3
e.	Arduino Nano board	3.9
f.	Voltage conversion module	0.7
	Sub total	**65.9**
2	**Solar charging module**	
a.	10 W solar panel	10.0
b.	Solar charge controller	3.3
c.	12 V battery	9.2

© 2025 The Author(s). | Published by Agro Intelligence Research Press

	Sub total	**22.5**
3	**Gateway unit**	
a.	LoRa communication module	13.3
b.	GSM communication module	10.7
c.	Microcontroller	3.2
d.	Buck converter	0.7
e.	Antenna	10.7
	Sub total	**38.6**
4	**Soil moisture sensor unit**	
a.	Capacitive soil moisture sensor	2.5
b.	LoRa module	13.3
c.	Microcontroller	3.2
d.	5 V Li-Ion battery	9.3
e.	Solar charger module	3.2
f.	PVC pipe	2.7
g.	Solar panel	0.9
	Sub total	**32.0**
	Overall total	**159.5 (approximately US$160)**

Assessment of automatic check gate

The automatic check gate was evaluated on its ability to open and close in response to preset soil moisture conditions, as well as its durability, energy use, and economic viability.

Power requirement

Solar energy from a solar photovoltaic module met the system's power needs. The setup proved highly energy-efficient, demanding minimal upkeep while ensuring reliable power availability even during cloudy conditions. A fully charged battery could run the check gate for three straight days without recharging if cloud cover persisted. The actuator, a 12 V DC motor with a 70 rpm gearbox, drew 2500 mA. The soil moisture sensor required 3.7-5.5 V (5 mA), while the gateway required 12 V. GSM operation required at least 1 A, and the microcontroller consumed 26 µA. Various parts of the check gate controller required a minimum of 5 V and 1 A to function. Even so, the check gate controller ran on a 12 V solar rechargeable battery. No power-related problems arose throughout the testing phase.

Cost of the system

Table 5 displays the cost breakdown for an automated irrigation system that includes four modules: the check gate and controller unit, solar charging module, gateway, and soil moisture sensor module. The estimated cost of the automated irrigation system was US$160.

Conclusion

© 2025 The Author(s). | Published by Agro Intelligence Research Press

An automatic check gate was created for basin irrigation and linked to IoT via a wireless soil moisture sensor network that uses GSM. The goal was to allow farmers or users to manage gate opening and closing remotely with minimal hands-on involvement. Farmers can access live field moisture data remotely and decide when to start and stop irrigation based on actual moisture readings. Successful trials took place in bare loamy soil. The research also explored optimal sensor positions and quantities in the field to improve irrigation application efficiency. Three operational schedules involving varied depth and length combinations along the water flow path were examined. These tests showed that at least 2 soil moisture sensors are required for effective system operation. One sensor, placed at a 15 cm depth and 50% of the field length, handles opening, while another manages closure. The optimal spot for the closing sensor is 37.5 cm depth at 25% of the length from the inlet under high soil moisture deficit, shifting to 7.5 cm depth at 75% of the length under low soil moisture deficit. This reveals that closing sensor placement varies with the level of soil moisture depletion. In general, automation raised average application efficiency to 86.6%. Both the hardware and software components functioned reliably across multiple situations. The automatic check gate demonstrated strong durability across various weather conditions (rainy, hot, winter) and required minimal upkeep. A web or mobile application enabled remote control to sustain target soil moisture levels with almost no manual effort. Solar energy supports sustainable power usage. Automation notably enhances application efficiency, reduces labor, enables remote access, and operates in real-time. In summary, the findings confirmed that the automatic check gate worked effectively alongside wireless sensors, leading to a marked rise in irrigation application efficiency via an IoT-based wireless soil moisture automatic basin irrigation setup. The outcomes point to promising potential for automation in surface irrigation to elevate irrigation efficiency.

Acknowledgements

The authors would like to thank ICAR- Indian Institute of Soil and Water Conservation, Dehradun, for granting study leave. We are thankful to the Water Technology Center, Farm Operation Service Unit (FOSU), ICAR-Indian Agricultural Research Institute, New Delhi, and M/S Agsmartic for providing all the research and experimental support.

Conflict of interest

None

Financial support

None

Ethics statement

None

Received: 29 Dec 2023 Revised: 03 Mar 2024 Accepted: 20 Mar 2024
Published online: 25 November 2025

Rights and permissions

Open Access The author(s) retain copyright. This article is licensed under the Creative Commons Attribution-NonCommercial-ShareAlike 4.0 International License. It may be shared and adapted for non-commercial purposes with appropriate attribution, an indication of changes, and distribution of adaptations under the same license. Third-party material may be subject to separate terms identified in its credit line. View the license at https://creativecommons.org/licenses/by-nc-sa/4.0/.

References

1. Dhawan V. Water and agriculture in India: Background paper for the South Asia Expert Panel during the Global Forum for Food and Agriculture (GFFA). Hamburg: OAV–German Asia-Pacific Business Association; 2017.

2. FAO. Water for sustainable food and agriculture: A report produced for the G20 Presidency of Germany. Rome: Food and Agriculture Organization of the United Nations; 2017.

3. Bjorneberg DL. Irrigation methods. Reference Module in Earth Systems and Environmental Sciences. Elsevier; 2013. ISBN: 9780124095489.
https://doi.org/10.1016/B978-0-12-409548-9.05195-2.

4. Government of India (GoI). Pocket book of agricultural statistics. New Delhi: Ministry of Agriculture and Farmers Welfare, Department of Agriculture, Cooperation & Farmers Welfare, Directorate of Economics and Statistics; 2017.

5. Smith RJ, Raine SR, Minkovich J. Irrigation application efficiency and deep drainage potential under surface irrigated cotton. Agric Water Manag. 2005;71(2):117–30.
https://doi.org/10.1016/j.agwat.2004.07.008.

6. Sivanappan RK. Status, scope and future prospects of micro-irrigation in India. In: Proceedings of the Workshop on Micro-Irrigation and Sprinkler Irrigation System; 1998; New Delhi, India. Central Board of Irrigation and Power (CBIP); 1998. p. 1–7.

7. Raine SR. The future of irrigation technologies and practices is here now. Keynote address. In: Proceedings of the Irrigation Australia 2006 Conference; 2006; Brisbane, Australia.

8. Clemmens AJ. Feedback control of basin irrigation system. J Irrig Drain Eng. 1992;118(3):480–96.
https://doi.org/10.1061/(ASCE)0733-9437(1992)118:3(480).

9. Smith RJ, Uddin M, Gillies MH, Clurey PM. Evaluating the performance of automated bay irrigation. Irrig Sci. 2016;34:175–85.
https://doi.org/10.1007/s00271-016-0494-8.

10. Michael RM, Hussain A, Gillies MH, Nicholas J. Inflow rate and border irrigation performance. Agric Water Manag. 2015;155:76–86.
https://doi.org/10.1016/j.agwat.2015.03.017.

11. Al-Ghobari HM, Mohammad FS, El Marazky MSA, Dewidar AZ. Automated irrigation systems for wheat and tomato crops in arid regions. Water SA. 2017;43(2):354–64.
https://doi.org/10.4314/wsa.v43i2.18.

12. Bowlekar AP, Patil ST, Kadam US, Mane MS, Nandgude SB, Palte NK. Performance evaluation of real-time automatic irrigation system on the yield of cabbage (Brassica oleracea L.). Int J Pure Appl Biosci. 2019;7:160–5.
https://doi.org/10.18782/2320-7051.7433.

13. Millán S, Casadesús J, Campillo C, Moñino MJ, Prieto MH. Using soil moisture sensors for automated irrigation scheduling in a plum crop. Water. 2019;11(10):2061.
https://doi.org/10.3390/w11102061.

14. Hardie M. Review of novel and emerging proximal soil moisture sensors for use in agriculture. Sensors. 2020;20(23):6934.
https://doi.org/10.3390/s20236934.

15. Vera J, Conejero W, Mira-García AB, Conesa MR, Ruiz-Sánchez MC. Towards irrigation automation based on dielectric soil sensors. J Hortic Sci Biotechnol. 2021;96(6):696–707.
https://doi.org/10.1080/14620316.2021.1906761.

© 2025 The Author(s). | Published by Agro Intelligence Research Press

16. Gutiérrez J, Villa-Medina JF, Nieto-Garibay A, Porta-Gándara MA. Automated irrigation system using a wireless sensor network and GPRS module. IEEE Trans Instrum Meas. 2014;63(1):166–76. https://doi.org/10.1109/TIM.2013.2276487.

17. Masseroni D, Moller P, Romani M, Tyrrell R, Lasagna A, Sali G, et al. Evaluating performances of the first automatic system for paddy irrigation in Europe. Agric Water Manag. 2018;201:58–69. https://doi.org/10.1016/j.agwat.2017.12.019.

18. Mandavia AB. Modernization of irrigation system operational management by way of canal automation in India. In: Proceedings of the 5th ITIS Network International Meeting on Modernization of Irrigation System Operations; Aurangabad, India. 1998.

19. Shingote KS, Shahane P. Microcontroller based flow control system for canal gates in irrigation canal automation. In: Proceedings of the IEEE 6th International Conference on Advanced Computing (IACC); 2016. p. 796–800. https://doi.org/10.1109/IACC.2016.152.

20. Sales N, Remédios O, Arsenio A. Wireless sensor and actuator system for smart irrigation on the cloud. In: Proceedings of the IEEE 2nd World Forum on Internet of Things (WF-IoT); 2015. p. 693–8. https://doi.org/10.1109/WF-IoT.2015.7389138.

21. Akyildiz IF, Kasimoglu IH. Wireless sensor and actor networks: Research challenges. Ad Hoc Netw. 2004;4(2):351–67. ISSN: 1570-8705. https://doi.org/10.1016/j.adhoc.2004.04.003.

22. Rodríguez-Robles J, Martín Á, Martín S, Ruipérez-Valiente JA, Castro M. Autonomous sensor network for rural agriculture environments: Low cost and energy self-charge. Sustainability. 2020;12(15):5913. https://doi.org/10.3390/su12155913.

23. Loukatos D, Arvanitis KG. Multi-Modal Sensor Nodes in Experimental Scalable Agricultural IoT Application Scenarios. In: Internet of Things and Edge Computing for Smart Agriculture. Springer, Cham; 2021. p. 101–28. https://doi.org/10.1007/978-3-030-71172-6_5.

24. Muangprathub J, Boonnam N, Kajornkasirat S, Lekbangpong N, Wanichsombat A, Nillaor P. IoT and agriculture data analysis for smart farm. Comput Electron Agric. 2019;156:467–74. https://doi.org/10.1016/j.compag.2018.12.011.

25. Lloret J, Sendra S, Garcia L, Jimenez JM. A wireless sensor network deployment for soil moisture monitoring in precision agriculture. Sensors. 2021;21(21):7243. https://doi.org/10.3390/s21217243.

26. Prasad AN, Mamun KA, Islam FR, Haqva H. Smart quality monitoring system. In: Proceedings of the 2nd Asia-Pacific World Congress on Computer Science and Engineering; 2015. p. 1–6.

27. Parameswaran G, Sivaprasath K. Arduino based smart drip irrigation system using Internet of Things. Int J Eng Sci Comput. 2016;6(5):5518–21. https://doi.org/10.4010/2016.1348.

28. Patil SJ, Patil A. Precision agriculture for water management using IoT. Int J Recent Innov Trends Comput Commun. 2017;5(12):142–4.

29. Shekhar Y, Dagur E, Mishra S, Tom RJ, Veeramanikandan M, Sankaranarayanan S. Intelligent IoT based automated irrigation system. Int J Appl Eng Res. 2017;12(18):7306–20.

30. Mehra M, Saxena S, Sankaranarayanan S, Tom RJ, Veeramanikandan M. IoT based hydroponics system using deep neural networks. Comput Electron Agric. 2018;155:473–86.

© 2025 The Author(s). | Published by Agro Intelligence Research Press

31. Nath S, Nath JK, Sarma PKC. IoT based system for continuous measurement and monitoring of temperature, soil moisture and relative humidity. Int J Electron Eng Technol. 2018;9(3):106–13.

32. Vuran MC, Salam A, Wong R, Irmak S. Internet of underground things: Sensing and communications on the field for precision agriculture. In: Proceedings of the IEEE World Forum on Internet of Things (WF-IoT); 2018. p. 586–91. https://doi.org/10.1109/WF-IoT.2018.8355228.

33. Singh SS. Smart irrigation system using IoT. Int J Innov Technol Explor Eng. 2019;8(12):183–6. https://doi.org/10.35940/IJITEE.L1054.10812S19.

34. Abioye EA, Abidin MSZ, Mahmud MSA, Buyamin S, Rahman A, Otuoze AO, et al. IoT-based monitoring and data-driven modelling of drip irrigation system for mustard leaf cultivation experiment. Inf Process Agric. 2021;8(2):270–83. https://doi.org/10.1016/j.inpa.2020.05.004.

35. Barman A, Neogi B, Pal S. Solar-powered automated IoT-based drip irrigation system. In: Pattnaik P, Kumar R, Pal S, Panda S, editors. IoT and Analytics for Agriculture. Studies in Big Data. Singapore: Springer; 2020;63: 23–47. https://doi.org/10.1007/978-981-13-9177-4_2.

36. Burt CM, Clemmens AJ, Solomon KH, Bliesner RD, Hardy LA, Howell TA, et al. Irrigation performance measures: Efficiency and uniformity. J Irrig Drain Eng. 1997;123(6):423–42. https://doi.org/10.1061/(ASCE)0733-9437(1997)123:6(423).

37. Merriam JL, Keller J. Farm Irrigation System Evaluation. 3rd ed. Logan, UT, USA: Agricultural and Irrigation Engineering Department, Utah State University; 1978.

38. Walker WR, Skogerboe GV. Surface Irrigation: Theory and Practice. Englewood Cliffs, NJ, USA: Prentice-Hall; 1987.

39. Sharma RK, Singh HR. Deep percolation losses in border-checks. J Soil Water Conserv. 2009;8(2):65–74.

40. Amiri Z, Gheysari M, Mosaddegh MR, Amiri S, Tabatabaei MS. An attempt to find a suitable place for soil moisture sensor in a drip irrigation system. Inf Process Agric. 2021. https://doi.org/10.1016/j.inpa.2021.04.010.

© 2025 The Author(s). | Published by Agro Intelligence Research Press